

Unfolding engineering metamaterials design: relaxed micromorphic modeling of large-scale acoustic meta-structures ¹

F. Erel-Demore ^a, G. Rizzi ^a, M. Collet ^b, P. Neff ^c, A. Madeo ^a

¹Institute for Structural Mechanics and Dynamics, Technical University Dortmund, Germany

²Laboratoire de Tribologie et de Dynamique des Systèmes, Ecole Centrale de Lyon, France

³Chair for Nonlinear Analysis and Modeling, University of Duisburg–Essen, Germany

¹Journal of the Mechanics and Physics of Solids, Volume 168, 2022, 104995, ISSN 0022-5096,
<https://doi.org/10.1016/j.jmps.2022.104995>

Introduction

Metamaterial (from $\mu\epsilon\tau\acute{\alpha}$, “beyond”): Architected material showing exotic mechanical characteristics that cannot be found in nature.

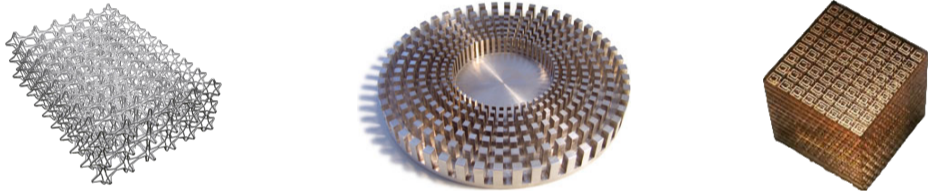


Figure 1: (left to right) (a) Foam with negative Poisson ratio [Lakes 1988]. (b) Seismic cloak [Guenneau 2014]. (c) Ultrasound Lense [Fang 2006].

Band-gap metamaterials inhibit wave propagation in particular frequency ranges.

Such effect can be achieved by:

- Bragg scattering
- local resonance

Modeling metamaterials: the relaxed micromorphic model

→ Such materials could be advantageously used in mechanical engineering

× Classical models are not suited for such structures

A homogenized model is required:

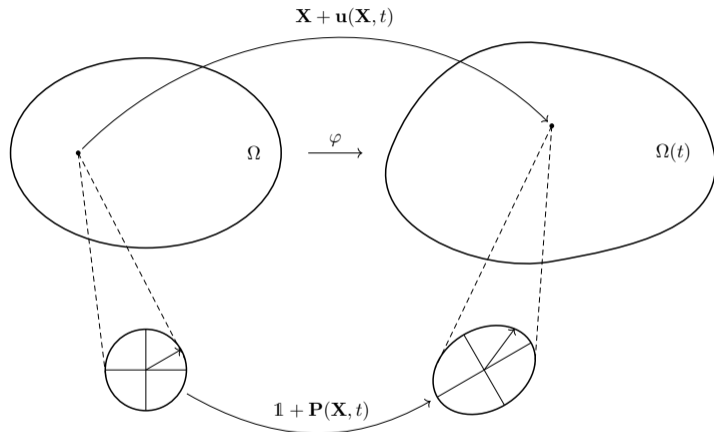
→ The relaxed micromorphic model allows such simplification



We present here:

- Design and manufacturing of such metastructures
- Experimental characterization and numerical modelling

Enriching the kinematic description of our media



Displacement: $\mathbf{u} = \begin{pmatrix} u_1 \\ u_2 \\ u_3 \end{pmatrix}$ Microdistorsion: $\mathbf{P} = \begin{pmatrix} P_{11} & P_{12} & P_{13} \\ P_{21} & P_{22} & P_{23} \\ P_{31} & P_{32} & P_{33} \end{pmatrix}$

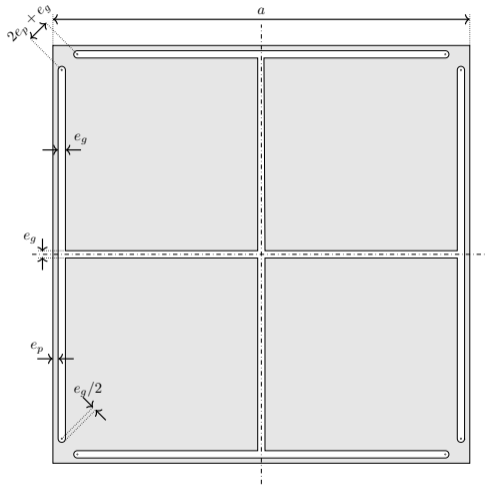
Lagrangian density of the relaxed micromorphic model

Generalized strain w_m and kinetic k_m energy density:

$$\begin{aligned}k_m(\dot{\mathbf{u}}, \nabla \dot{\mathbf{u}}, \dot{\mathbf{P}}) &= \frac{1}{2} \langle \dot{\mathbf{u}}, \rho_m \dot{\mathbf{u}} \rangle \text{ (Cauchy inertia)} \\ &+ \frac{1}{2} \langle \text{sym } \dot{\mathbf{P}}, \mathbb{J}_m \text{sym } \dot{\mathbf{P}} \rangle + \frac{1}{2} \langle \text{skew } \dot{\mathbf{P}}, \mathbb{J}_c \text{skew } \dot{\mathbf{P}} \rangle \text{ (free micro-inertia)} \\ &+ \frac{1}{2} \langle \text{sym } \nabla \dot{\mathbf{u}}, \mathbb{T}_e \text{sym } \nabla \dot{\mathbf{u}} \rangle + \frac{1}{2} \langle \text{skew } \nabla \dot{\mathbf{u}}, \mathbb{T}_c \text{skew } \nabla \dot{\mathbf{u}} \rangle \text{ (gradient micro-inertia)} \\ w_m(\nabla \mathbf{u}, \mathbf{P}) &= \frac{1}{2} \langle \text{sym}(\nabla \mathbf{u} - \mathbf{P}), \mathbb{C}_e \text{sym}(\nabla \mathbf{u} - \mathbf{P}) \rangle \text{ (elastic energy)} \\ &+ \frac{1}{2} \langle \text{sym } \mathbf{P}, \mathbb{C}_m \text{sym } \mathbf{P} \rangle \text{ (micro self energy)} \\ &+ \frac{1}{2} \langle \text{skew}(\nabla \mathbf{u} - \mathbf{P}), \mathbb{C}_c \text{skew}(\nabla \mathbf{u} - \mathbf{P}) \rangle \text{ (local rotational elastic coupling)}\end{aligned}$$

→ Systems are modeled by the introduction of an appropriate Action

The metamaterial unit cell



a	20	[mm]
e_g	0.35	[mm]
e_p	0.25	[mm]
ρ_{Ti}	4400	[kg/m ³]
E_{Ti}	112	[GPa]
ν_{Ti}	0.34	-

Figure 2: (left) Geometry of the architected cell with its parametrization and (right) its mechanical properties (titanium alloy TA6V).

Fitting of the dispersion curves

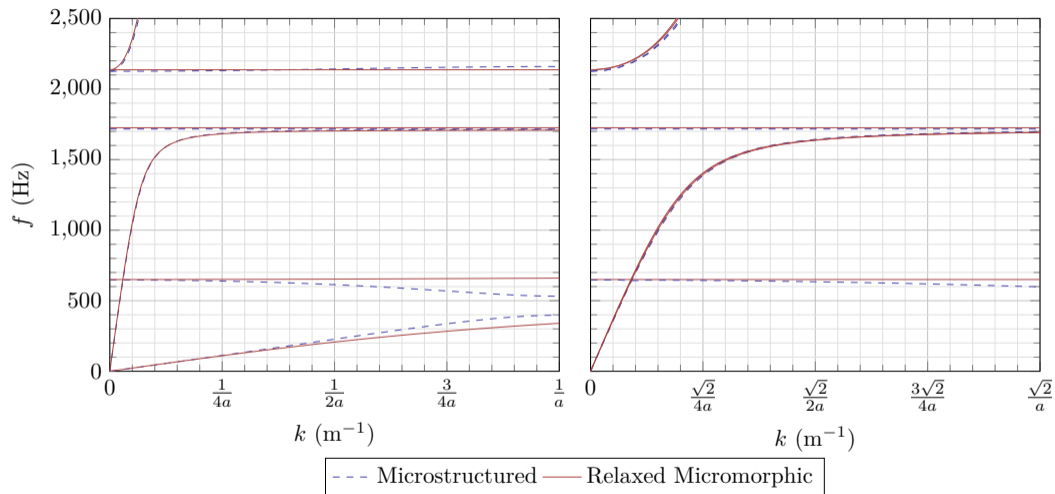
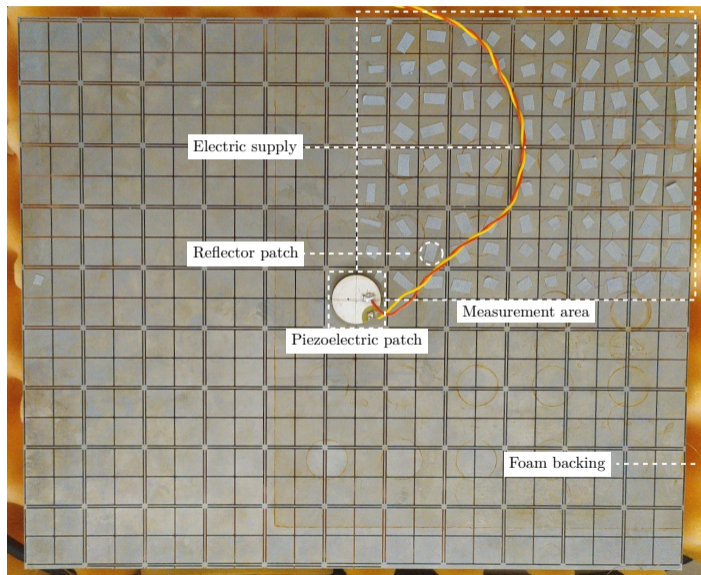
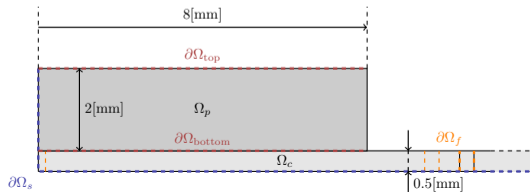
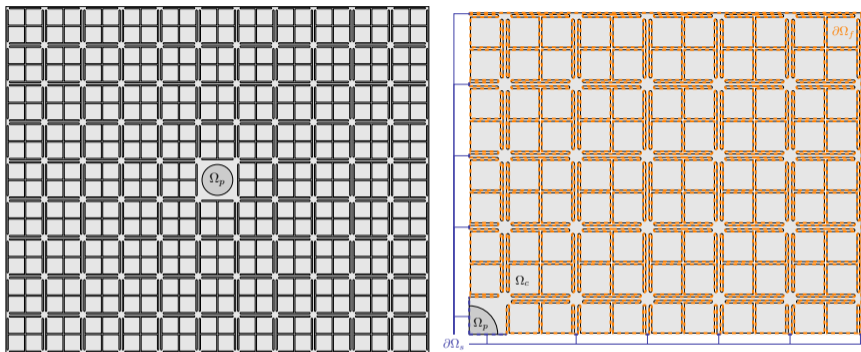


Figure 3: Dispersion curves of the microstructured and the relaxed micromorphic systems along ΓX (left, propagation at 0°) and ΓM (right, propagation at 45°).

Experimental set-up of the *proof-of-concept*



Comparison with the experiment: the microstructured plate



Modelling the microstructured plate

Action functional of the system:

$$\mathcal{A}_{\text{int}}[\mathbf{u}, V] = \int_{t_1}^{t_2} \left[\int_{\Omega_p} (k_p - w_p - q) dx_1 dx_2 dx_3 + \frac{e}{2} \int_{\Omega_c} (k_c - w_c) dx_1 dx_2 \right] dt$$

Plain strain hypothesis in the microstructured plate:

$$\mathbf{u} = \begin{pmatrix} u_1 \\ u_2 \\ 0 \end{pmatrix} \text{ in } \Omega_c, \quad \mathbf{u} = \begin{pmatrix} u_1 \\ u_2 \\ u_3 \end{pmatrix} \text{ in } \Omega_p \text{ and } u_3 = 0 \text{ on } \Omega_{\text{bottom}}$$

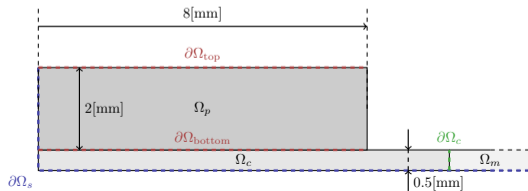
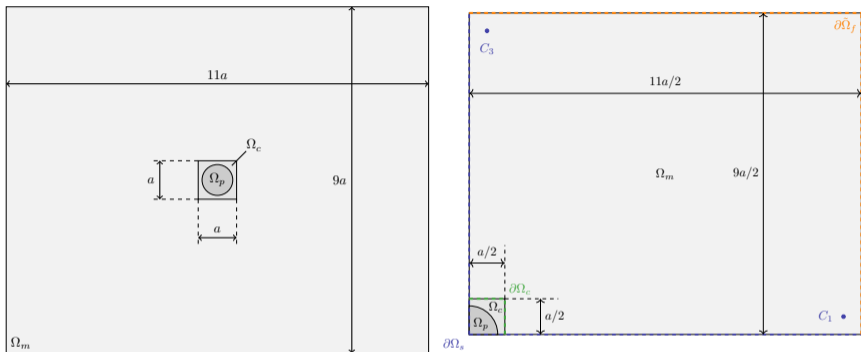
Piezoelectric excitation and symmetry conditions:

$$\begin{cases} V = 0 & \text{on } \partial\Omega_{\text{bottom}} \\ V = V_0 & \text{on } \partial\Omega_{\text{top}} \end{cases} \quad \text{and} \quad \begin{cases} \langle \mathbf{u}, \mathbf{n} \rangle = 0 \\ \langle \mathbf{D}, \mathbf{n} \rangle = 0 \end{cases} \quad \text{on } \partial\Omega_s$$

Computation of the FRF under Comsol:

$$FRF(\mathbf{x}) = \frac{|\dot{\mathbf{u}}|}{V_0} \quad \text{on } \mathbf{x} = C_1 = (0.105, 0.005) \text{ [m]}$$

Modelling for the relaxed micromorphic medium



Action functional of the relaxed micromorphic model

Action functional of the system:

$$\mathcal{A}_{\text{int}}[\mathbf{u}, \mathbf{P}, V] = \int_{t_1}^{t_2} \left[\int_{\Omega_p} (k_p - w_p - q) d\Omega + \frac{e}{2} \int_{\Omega_c} (k_c - w_c) d\Gamma \right] dt \\ + \frac{e}{2} \int_{t_1}^{t_2} \int_{\Omega_m} (k_m - w_m) d\Gamma dt$$

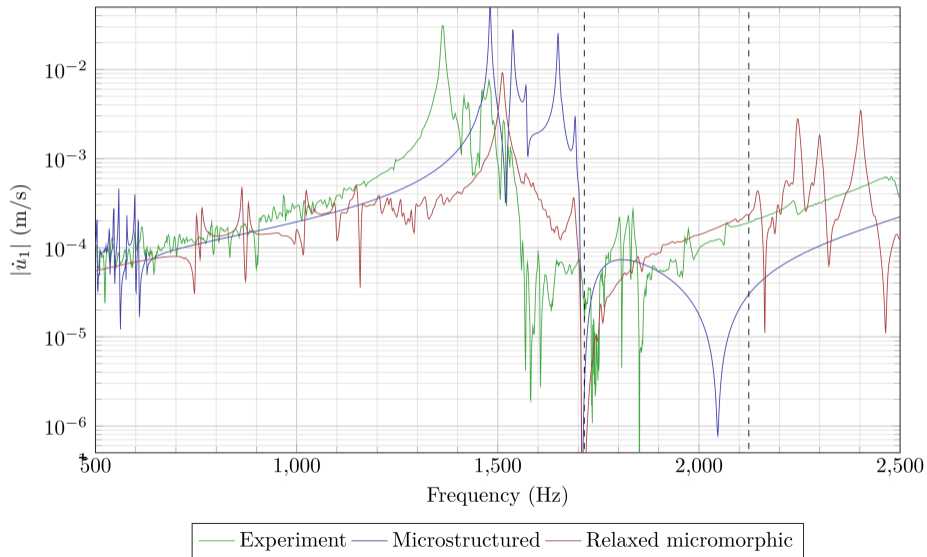
Plane strain hypothesis in the plate:

$$\mathbf{u} = \begin{pmatrix} u_1 \\ u_2 \\ u_3 \end{pmatrix} \text{ in } \Omega_p, \mathbf{u} = \begin{pmatrix} u_1 \\ u_2 \\ 0 \end{pmatrix} \text{ in } \Omega_c, \mathbf{u} = \begin{pmatrix} u_1 \\ u_2 \\ 0 \end{pmatrix} \text{ and } \mathbf{P} = \begin{pmatrix} P_{11} & P_{12} & 0 \\ P_{21} & P_{22} & 0 \\ 0 & 0 & 0 \end{pmatrix} \text{ in } \Omega_m$$

Traction-free and symmetry boundary conditions:

$$\begin{cases} (\hat{\sigma}_{ij} + \tilde{\sigma}_{ij})n_j = 0 & \text{on } \partial\tilde{\Omega}_f \\ (\hat{\sigma}_{ij} + \tilde{\sigma}_{ij})n_j = \sigma_{ij}^c n_j & \text{on } \partial\Omega_c \end{cases} \text{ and } \begin{cases} u_i n_i = 0 \\ (\delta_{ki} - n_k n_i)(P_{ij} n_j) = 0 \end{cases} \text{ on } \partial\Omega_s$$

Comparison with the experiment in C_1



Recalibration and perturbation of the model

- × Shift between the theoretical FRFs and the experimental one
- × Theoretical band gap “deeper” than the experimental one

→ Reconsider the hypotheses made in the framework of our modelling:

- linear hypothesis
- idealized geometry
- plane strain hypothesis
- idealized constitutive laws
- idealized boundary conditions

→ Recalibration of the parameters:

$$E^{\text{recalibration}} = (1 + \kappa_w)E_{Ti} \quad \text{and} \quad \rho_c^{\text{recalibration}} = (1 + \kappa_k)\rho_{Ti}$$

→ Perturbation (θ_ρ and θ_E follow a zero-mean probability law):

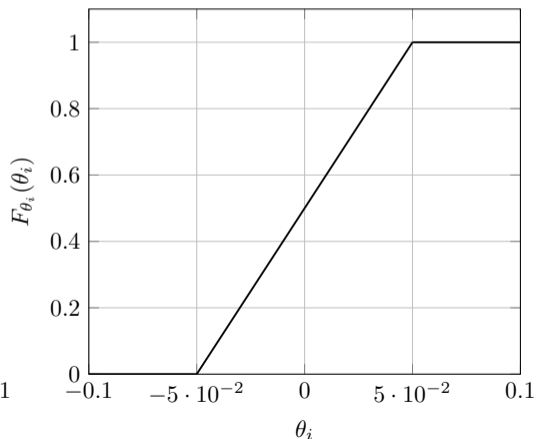
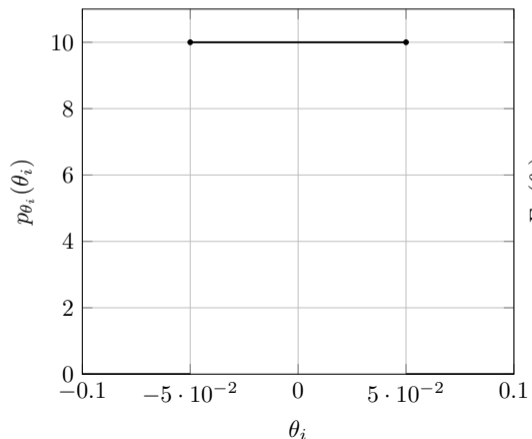
$$\begin{cases} \rho_c(\mathbf{x}) = (1 + \theta_\rho(\mathbf{x}))\rho_c^{\text{recalibration}} = (1 + \theta_\rho(\mathbf{x}))(1 + \kappa_k)\rho_{Ti} \\ E(\mathbf{x}) = (1 + \theta_E(\mathbf{x}))E^{\text{recalibration}} = (1 + \theta_E(\mathbf{x}))(1 + \kappa_w)E_{Ti} \end{cases}$$

Recalibration and perturbations chosen

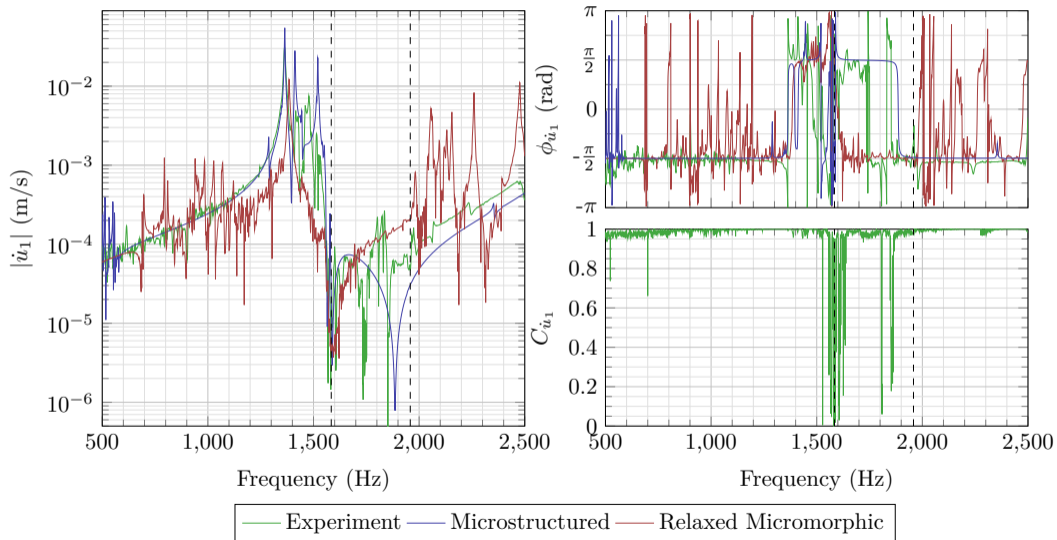
→ Optimal values of recalibration parameters:

$$\kappa_k = +0.05 \quad \text{and} \quad \kappa_w = -0.10875 \quad (1)$$

→ Continuous uniform distribution used for both models:



Test/computation comparison of \dot{u}_1 at C_1



Response of the plate at 1589 Hz

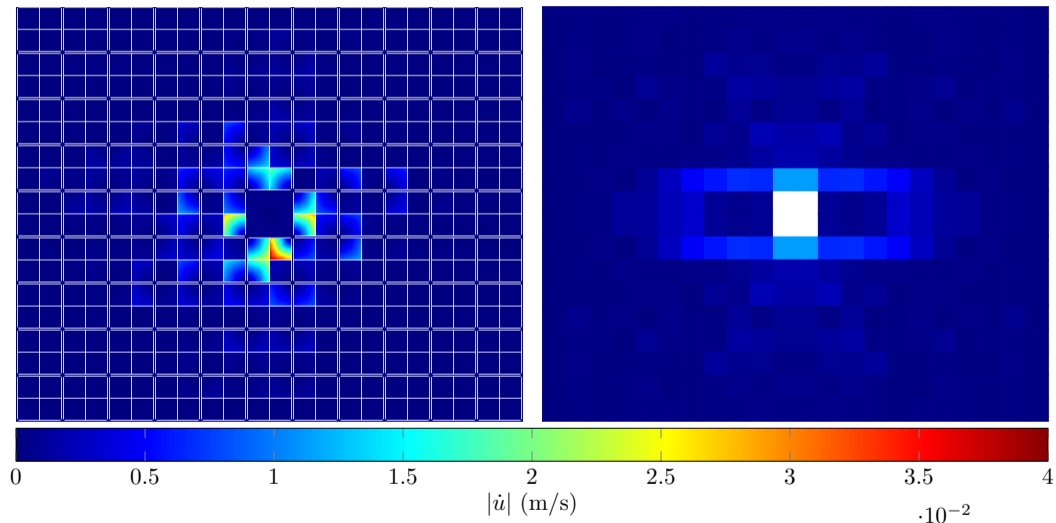


Figure 4: $|\dot{\mathbf{u}}|$ for the microstructured model (*left*) and for the symmetrized experiment (*right*). 17/18

Conclusions and perspectives

Achievements:

- Design and characterization of a metastructure with band-gap
- Numerical validation of the relaxed micromorphic model
- Integration of metamaterials in new structures
- Successful comparison with the experiment:
 Manufacturing defects taken into account

Perspectives:

- Manufacturing of energy focusing metastructures
- Take into account mechanical damping
- Improvement of the perturbation procedure:
 Limited to the band-gap frequencies

Thank you for your attention!

Questions?